Hierarchical Microstructures

DOI: 10.1002/anie.201300190

Self-Supported Construction of Uniform Fe_3O_4 Hollow Microspheres from Nanoplate Building Blocks

*Bao Wang, Hao Bin Wu, Lei Zhang, and Xiong Wen (David) Lou**

Hollow structures have attracted increasing attention because of their promising use in a wide range of important applications, such as water treatment, catalysis, sensors, drug delivery, and energy storage.[1–4] Over the past decade, numerous hollow structures with different features have been synthesized to meet the demands of many scientific and technological applications, as the performance of hollow structures depends not only on their composition but also on many other structural features, such as the size and morphology of the particles.[5–11]

Despite the intense effort that has been made, it is still a big challenge to develop facile and reliable methods for the controlled synthesis of hollow structures in terms of their size, morphology, and components. Templating methods have been widely used to generate many hollow structures. However, they are quite tedious and costly, as the process generally involves several steps, including the preparation of templates, the deposition of shell materials (or precursors) onto the templates, and finally the removal of the templates by harsh chemical procedures.[1,12–14] In particular, partial collapse of the hollow structures upon template removal appears inevitable. This problem becomes more serious when nanosized building blocks are used to construct microsized hollow structures. The self-assembly of nanosized building blocks, followed by inside-out Ostwald ripening, is considered one of most efficient methods for the preparation of hollow structures.[15,16] Synthesis systems based on ethylene glycol (EG) have been widely adopted for the preparation of metal-oxide nanostructures.[17,18] Recently, Co_3O_4 hollow structures were obtained from EG-based systems in the presence of large amounts of poly(vinylpyrrolidone) (PVP).[19] In such synthesis systems, EG (or its derivative) serves not only as the solvent, but also sometimes as a complexing agent.

Herein, we report a facile solvothermal method for the construction of hierarchical hollow microspheres from nanoplate building blocks. In this simple synthesis, EG was used as the solvent and ethylenediamine (EDA) as an additive. An interesting structural evolution from solid microspheres to hollow microspheres composed of nanoplates was observed. These iron-containing hollow microspheres were subsequently converted into magnetic Fe_3O_4 hollow microspheres without significant structural alteration. The as-obtained Fe_3O_4 hollow microspheres exhibited high reversible capacity and excellent cycling performance as an anode material for lithium-ion batteries (LIBs).

The chemical composition of the calcined product was determined by X-ray diffraction (XRD) analysis. All diffraction peaks in the XRD pattern could be unambiguously assigned to the Fe_3O_4 phase (JCPDS card no. 65-3107; Figure 1a). The morphology of the Fe_3O_4 particles obtained was observed by field emission scanning electron microscopy (FESEM). The FESEM image (Figure 1b) showed that the product was composed of uniform spherical particles with a diameter of approximately 5 μm. From some broken microspheres (see Figure 1c), it could also be clearly seen

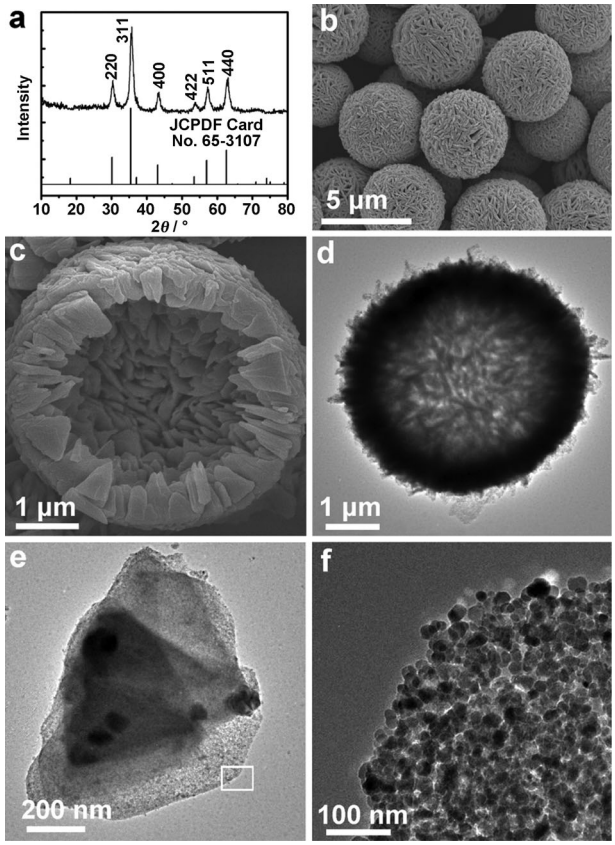

Figure 1. a) XRD pattern, b,c) FESEM images, and d–f) TEM images of the as-obtained Fe_3O_4 hollow microspheres. Image (f) is a magnified view of the area marked by a rectangle in (e).

[*] Dr. B. Wang, H. B. Wu, Dr. L. Zhang, Prof. X. W. Lou
School of Chemical and Biomedical Engineering
Nanyang Technological University
62 Nanyang Drive, Singapore 637459 (Singapore)
E-mail: xwlou@ntu.edu.sg
Homepage: http://www.ntu.edu.sg/home/xwlou
Dr. B. Wang, H. B. Wu
School of Materials Science and Engineering
Nanyang Technological University
50 Nanyang Avenue, Singapore 639798 (Singapore)

Supporting information for this article is available on the WWW under http://dx.doi.org/10.1002/anie.201300190.

that the spheres were hollow and composed of densely packed platelike subunits. The hollow interior of these spheres was further characterized by transmission electron microscopy (TEM; Figure 1 d), which showed them to have a large void space and a well-defined shell. From the FESEM (Figure 1 c) and TEM images (Figure 1 e), it can be seen that the platelike subunits are wedge-shaped and thus give a certain curvature to facilitate the construction of the spherical structure. A TEM image (Figure 1 f) taken of the area marked with a white rectangle in Figure 1 e showed that the nanoplates were porous and composed of small nanoparticles.

The uncalcined precursor particles obtained in the presence of EDA (2 mL) in the reaction mixture were characterized by FESEM and TEM (see Figure S1 in the Supporting Information). When the morphologies of the precursor and final Fe_3O_4 particles are compared, there appears to be no noticeable structural change caused by the calcination process. The XRD pattern (see Figure S2) of the precursor particles showed diffraction peaks similar to those of a previously described product, which was presumably iron alkoxide.[20] The CH_2- vibrational bands at approximately 2880 and 2840 cm^{-1} and the C–OH stretching band at 1080 cm^{-1} in the Fourier transform infrared (FTIR) spectrum (see Figure S3) are also identical to the reported bands. We therefore concluded that the as-synthesized iron-containing precursor was probably iron alkoxide,[17,18,21] although the exact crystal structure of the precursor has not yet been determined.

In the present simple solvothermal system, the EDA additive was found to play a critical role in the formation of precursor particles: no precipitate was formed in the absence of EDA. We therefore investigated the effect of EDA in the reaction mixture on the product morphology. When less EDA was used, the particles obtained were hollow spheres with a smaller hollow interior (1.4 mL of EDA) and flowerlike structures (0.7 mL of EDA; see Figure S4). It was also observed that the size of the platelike subunits increased when less EDA was present in the reaction system. In the presence of 3 mL of EDA, the particles obtained were composed of several even larger nanoplates, and some of the particles contained a hole in the center (see Figure S5). When the amount of EDA was increased further to more than 4 mL, there was again no precipitate formed. These observations suggest that the formation of hollow spheres composed of nanoplates depends primarily on the concentration of EDA in the reaction system.

We next carried out a time-dependent experiment to investigate the formation of hollow microspheres in the present system. Only nanoparticles were collected after a reaction time of 1 h (see Figure S6). When the reaction duration was prolonged to 2 h, spheres with plate-like subunits were formed (see Figure S7). Figure 2 a illustrates the formation process of the precursor hollow spheres. Small nanoparticles initially formed will self-assemble into solid spheres comprised of platelike subunits. During a longer reaction time, the small crystallites in the core region of the sphere are selectively dissolved according to a well-known inside-out Ostwald ripening process.[1,16] The hollowing process continues with longer reaction times until well-defined hollow spheres comprising nanoplates are formed. The TEM images in Figure 2 b–e reveal the interesting hollowing process. The spheres obtained after reaction for 2 h were completely solid (Figure 2 b). When the reaction time was extended to 4 h, a hollowing effect started to appear around the central region of the spheres (Figure 2 c). The size of the interior void of the spheres increased further with longer reaction times. When the reaction duration was prolonged to more than 8 h, well-defined hollow spheres were finally created (Figure 2 d,e).

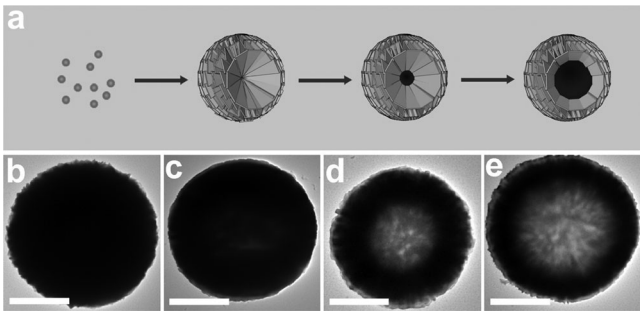

Figure 2. a) Schematic illustration of the formation process of the hollow microspheres. b–e) TEM images of the products obtained after reaction for b) 2 h, c) 4 h, d) 8 h, and e) 16 h. Scale bars: 2 μm.

The thermal decomposition of presynthesized precursor nanostructures is a simple way to obtain tailored metal-oxide nanostructures.[22] Thermogravimetric analysis (TGA) of the precursor hollow spheres showed that a weight loss of about 40 % occurred between 250 and 500 °C under a flow of N_2 (see Figure S8). Some interparticle mesopores will be generated during the thermal decomposition. The N_2 adsorption–desorption isotherm of as-obtained Fe_3O_4 hollow microspheres is shown in Figure S9 (see the Supporting Information). A relatively high Brunauer–Emmett–Teller (BET) specific surface area of about 78 $m^2 g^{-1}$ with a broad pore-size distribution was found for the uniform Fe_3O_4 hollow microspheres, in agreement with the porous texture of the shell.

Iron oxides have been widely studied as potential high-capacity anode materials for LIBs.[23–27] Electrochemical lithium storage in iron oxides follows the conversion reaction mechanism described by Equation (1):[28,29]

$$FeO_x + 2x\,Li^+ + 2x\,e^- \leftrightarrow x\,Li_2O + Fe \quad (1)$$

The formation of Li_2O and Fe in the forward reaction is thermodynamically favorable during the discharge process. However, the extraction of Li^+ ion from Li_2O in the reverse process is more difficult, which suggests that a certain extent of irreversibility is inevitable. It is known that many characteristics of nanoparticles, such as their structure, size and shape, have crucial effects on the electrochemical performance. Microsized structures assembled from nanosized building blocks might inherit the advantages of enhanced electrochemical reactivity from the nanosized building blocks and improved structural stability and packing density from the secondary microsized structure.

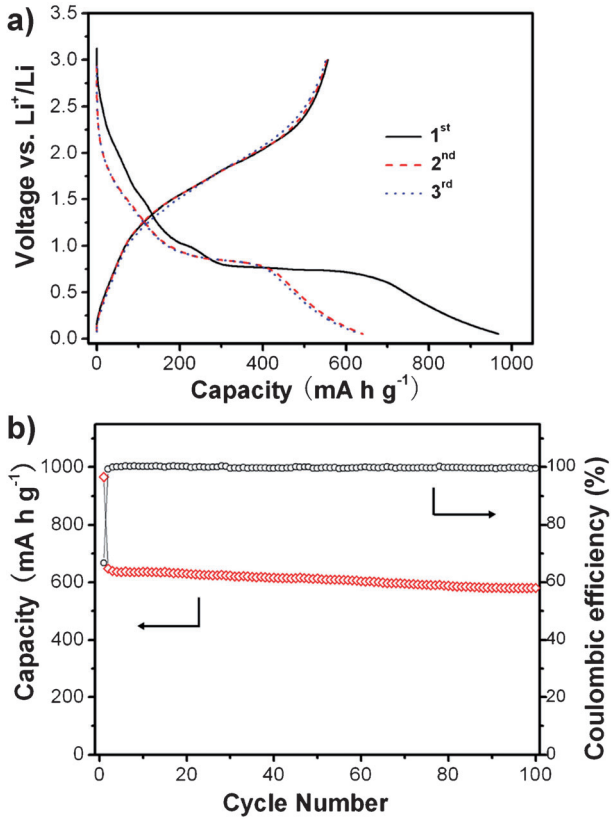

Figure 3. a) Discharge–charge voltage profiles and b) cycling performance of the Fe_3O_4 hollow spheres. All galvanostatic tests were performed at a constant current density of 200 mA g^{-1} between 0.05 and 3.0 V.

We investigated the electrochemical lithium-storage properties of the as-prepared Fe_3O_4 hollow microspheres. The charge–discharge voltage profiles of the sample are shown in Figure 3a. A distinct voltage plateau could be clearly identified at about 0.75 V, which is consistent with that found in reported studies.[30,31] This conversion reaction provides the dominant contribution to the lithium-storage capacity of the material and gives rise to a high initial discharge capacity of 960 mA h g^{-1}. A reversible charge capacity of 640 mA h g^{-1} can be delivered, which leads to a relatively low irreversible capacity loss of 33%. Such initial irreversible capacity loss is commonly ascribed to the formation of solid–electrolyte interface (SEI) and some other side reactions. However, the moderate surface area of the hollow microspheres limits irreversible surface reactions. The Coulombic efficiency increases rapidly to 98% in the second cycle. The cycling performance together with the Coulombic efficiency of the sample is depicted in Figure 3b at a constant current density of 200 mA g^{-1} between 0.05 and 3.0 V. From the second cycle onwards, the as-prepared Fe_3O_4 hollow spheres exhibit excellent cyclic capacity retention with a stable capacity of about 640 mA h g^{-1}. At the end of 100 charge–discharge cycles, a reversible capacity as high as 580 mA h g^{-1} can still be retained. The ultrahigh specific capacity of the Fe_3O_4 hollow spheres steadily decreases as the current rate increases (see Figure S10), probably as a result of the slow diffusion of Li^+ ions in the solid material.

Such remarkable electrochemical performance, especially the high specific capacity at low current rates and enhanced cycling stability, might be related to the advantageous structure of these hollow spheres. Specifically, we postulate that these hollow microspheres formed by a self-supported transformation route should have high structural integrity. Moreover, the nanoplate building blocks and the hollow interior can provide efficient transport of Li^+ ions because of the short diffusion length and the high porosity. Despite the reduced volumetric capacity due to the empty space in the hollow spheres, these Fe_3O_4 microspheres have potential as an interesting anode material.

In summary, we have developed a simple ethylenediamine-mediated solvothermal method for the synthesis of iron-containing hollow microspheres composed of nanoplates. The initially formed microspheres were observed to undergo an interesting hollowing process. These precursor hollow microspheres can be readily converted into Fe_3O_4 hollow microspheres by thermal decomposition under a N_2 atmosphere without significant structural collapse. In view of their unique structural advantages, these as-prepared Fe_3O_4 hollow microspheres were evaluated as an anode material for lithium-ion batteries. Their electrochemical characterization showed significantly improved lithium-storage capabilities with a very high reversible capacity of 580 mA h g^{-1} even after 100 cycles.

Experimental Section

Materials preparation: The precursor hollow microspheres were synthesized by a simple solvothermal method. All chemicals were of analytical grade and used as received without further purification. In a typical synthesis, $FeCl_3{\cdot}6H_2O$ (ca. 0.21 g; Sigma–Aldrich, 99.9%) was dissolved in a mixture of ethylene glycol (38 mL) and ethylenediamine (2 mL). The resulting mixture was stirred for 30 min and then transferred into a 50 mL Teflon-lined stainless-steel autoclave, which was heated at 150 °C for a period of 24 h in an electric oven. The autoclave was then allowed to cool down naturally to room temperature. The precipitate was collected and washed with ethanol several times by centrifugation, then dried at 60 °C overnight. The as-synthesized intermediate product was then transformed into Fe_3O_4 by calcination at 450 °C under a flow of N_2 for 2 h at a ramping rate of 1 °C min^{-1}.

Materials characterization: The chemical composition of the product was characterized by X-ray diffraction (XRD, Bruker, D8-Advance X-ray Diffractometer, $Cu_{K\alpha}$ radiation, $\lambda = 1.5406$ Å). The morphology of the synthesized products was examined by FESEM (JEOL, JSM-6700F, 5 kV) and TEM (JEOL, JEM-2010, 200 kV). The N_2 adsorption–desorption isotherm was obtained by using a Quantachrome Instruments Autosorb AS-6B instrument. The thermal behavior of the samples was characterized by TGA (Shimadzu TGA-60) at a ramping rate of 10 °C min^{-1} from room temperature to 600 °C in a dynamic atmosphere of N_2 (200 mL min^{-1}) by using an alumina crucible.

Electrochemical measurements: Electrochemical tests were carried out by using two-electrode Swagelok-type cells with pure lithium foil as the counter and also the reference electrode at room temperature. The working electrode was composed of a mixture of the active material, conducting carbon black (Super-P-Li), and a polymer binder (poly(vinylidene difluoride)) in a weight ratio of 80:10:10. The electrolyte used was 1.0 M $LiPF_6$ in a 50:50 (w/w)

mixture of ethylene carbonate and diethyl carbonate. Cells were assembled in an argon-filled glove box with the moisture and oxygen content maintained below 1.0 ppm. Cyclic voltammetry and galvanostatic charge–discharge measurements were performed by using a CHI electrochemical workstation and a Neware battery tester, respectively.

Received: January 9, 2013
Published online: March 13, 2013

Keywords: anode materials · hollow microspheres · iron oxides · lithium-ion batteries · self-assembly

[1] X. W. Lou, L. A. Archer, Z. C. Yang, *Adv. Mater.* **2008**, *20*, 3987.
[2] Z. Y. Wang, L. Zhou, X. W. Lou, *Adv. Mater.* **2012**, *24*, 1903.
[3] J. Hu, M. Chen, X. Fang, L. Wu, *Chem. Soc. Rev.* **2011**, *40*, 5472.
[4] X. Y. Lai, J. E. Halpert, D. Wang, *Energy Environ. Sci.* **2012**, *5*, 5604.
[5] P. M. Arnal, M. Comotti, F. Schuth, *Angew. Chem.* **2006**, *118*, 8404; *Angew. Chem. Int. Ed.* **2006**, *45*, 8224.
[6] M. Yang, J. Ma, C. L. Zhang, Z. Z. Yang, Y. F. Lu, *Angew. Chem.* **2005**, *117*, 6885; *Angew. Chem. Int. Ed.* **2005**, *44*, 6727.
[7] W. Feng, L. D. Sun, Y. W. Zhang, C. H. Yan, *Small* **2009**, *5*, 2057.
[8] J. S. Chen, J. Liu, S. Z. Qiao, R. Xu, X. W. Lou, *Chem. Commun.* **2011**, *47*, 10443.
[9] B. Liu, H. C. Zeng, *J. Am. Chem. Soc.* **2004**, *126*, 8124.
[10] Y. H. Deng, H. Tuysuz, J. Henzie, P. D. Yang, *Small* **2011**, *7*, 2037.
[11] J. B. Joo, Q. Zhang, I. Lee, M. Dahl, F. Zaera, Y. D. Yin, *Adv. Funct. Mater.* **2012**, *22*, 166.
[12] F. Caruso, R. A. Caruso, H. Möhwald, *Science* **1998**, *282*, 1111.
[13] S. W. Kim, M. Kim, W. Y. Lee, T. Hyeon, *J. Am. Chem. Soc.* **2002**, *124*, 7642.
[14] Z. Z. Yang, Z. W. Niu, Y. F. Lu, Z. B. Hu, C. C. Han, *Angew. Chem.* **2003**, *115*, 1987; *Angew. Chem. Int. Ed.* **2003**, *42*, 1943.
[15] A. Q. Pan, H. B. Wu, L. Yu, X. W. Lou, *Angew. Chem.* **2013**, *125*, 2282; *Angew. Chem. Int. Ed.* **2013**, *52*, 2226.
[16] X. W. Lou, Y. Wang, C. L. Yuan, J. Y. Lee, L. A. Archer, *Adv. Mater.* **2006**, *18*, 2325.
[17] X. C. Jiang, Y. L. Wang, T. Herricks, Y. N. Xia, *J. Mater. Chem.* **2004**, *14*, 695.
[18] Y. L. Wang, X. C. Jiang, Y. N. Xia, *J. Am. Chem. Soc.* **2003**, *125*, 16176.
[19] X. Wang, X. L. Wu, Y. G. Guo, Y. T. Zhong, X. Q. Cao, Y. Ma, J. N. Yao, *Adv. Funct. Mater.* **2010**, *20*, 1680.
[20] L. S. Zhong, J. S. Hu, H. P. Liang, A. M. Cao, W. G. Song, L. J. Wan, *Adv. Mater.* **2006**, *18*, 2426.
[21] A. M. Cao, J. S. Hu, H. P. Liang, L. J. Wan, *Angew. Chem.* **2005**, *117*, 4465; *Angew. Chem. Int. Ed.* **2005**, *44*, 4391.
[22] D. Larcher, G. Sudant, R. Patrice, J. M. Tarascon, *Chem. Mater.* **2003**, *15*, 3543.
[23] W. M. Zhang, X. L. Wu, J. S. Hu, Y. G. Guo, L. J. Wan, *Adv. Funct. Mater.* **2008**, *18*, 3941.
[24] B. Wang, J. S. Chen, H. B. Wu, Z. Wang, X. W. Lou, *J. Am. Chem. Soc.* **2011**, *133*, 17146.
[25] J. E. Lee, S. H. Yu, D. J. Lee, D. C. Lee, S. I. Han, Y. E. Sung, T. Hyeon, *Energy Environ. Sci.* **2012**, *5*, 9528.
[26] Z. Y. Wang, D. Y. Luan, S. Madhavi, Y. Hu, X. W. Lou, *Energy Environ. Sci.* **2012**, *5*, 5252.
[27] H. B. Wu, J. S. Chen, H. H. Hng, X. W. Lou, *Nanoscale* **2012**, *4*, 2526.
[28] P. Poizot, S. Laruelle, S. Grugeon, L. Dupont, J. M. Tarascon, *Nature* **2000**, *407*, 496.
[29] J. Cabana, L. Monconduit, D. Larcher, M. R. Palacin, *Adv. Mater.* **2010**, *22*, E170.
[30] L. Li, T. T. Wang, L. Y. Zhang, Z. M. Su, C. G. Wang, R. S. Wang, *Chem. Eur. J.* **2012**, *18*, 11417.
[31] J. S. Chen, Y. M. Zhang, X. W. Lou, *ACS Appl. Mater. Interfaces* **2011**, *3*, 3276.

